Kupczak *et al. Heritage Science* (2024) 12:49
https://doi.org/10.1186/s40494-024-01171-y

Heritage Science

RESEARCH

Open Access

The use of predominance area diagrams (PAD) to determine the oxygen and sulfur fugacities prevailing during historical metallurgical processes: the case of fifteenth to seventeenth century copper slags from Polichno (Old Polish industrial district)

Krzysztof Kupczak[1*], Rafał Warchulski[1], Aleksandra Gawęda[1], Marta Ślęzak[2] and Piotr Migas[2]

Abstract

The study presents the first use of predominance area diagrams (PADs) to determine oxidation–reduction conditions during reconstructing historical copper smelting processes. The smelting temperature and oxygen and sulfur fugacities during smelting were determined based on experiments and the geochemical (ICP-MS/ES, XRF) and mineralogical (SEM, EPMA) analyses of the fifteenth to seventeenth century slags from Polichno (Holy Cross Mountains, Poland). Results obtained during high-temperature experiments allowed to determine the slags' solidus and liquidus temperatures. The liquidus temperature was in the range of 1100–1200 °C, and the solidus temperature was in the range of 800–1100 °C. Data on temperature conditions were used in thermodynamic calculations to construct predominance area diagrams and then to determine the ranges of oxygen and sulfur fugacities in which the formation of slags was possible. Slags from Polichno were formed with the oxygen fugacity in the range of $\log P_{O_2} = -4.30$ (POL1, POL4 at 1200 °C) to −14.08 atm. (POL3 at 1090 °C). In turn, the sulfur fugacity during slag formation ranged from $\log P_{S_2} = -2.50$ (POL5 at 1200 °C) to −6.92 (POL4 at 1060 °C) atm. The relatively high sulfur availability confirms using sulfide ores without prior roasting. The wide range of sulfur and oxygen fugacity indicates the process's heterogeneity.

Keywords Slags, Predominance area diagrams, Process reconstruction, Smelting, Temperature

Introduction

Smelting slags are materials from which a lot of information can be obtained about historical metal production processes. Based on the chemical and phase compositions, it is possible to determine the slags' liquidus (complete melting of the material) and solidus (the beginning of the melting process) temperatures, the viscosity of the metallurgical melt, the batch composition, the oxidation–reduction conditions under which the smelting took place, and to decipher the reactions occurring during the process [1–10]. Temperature is the crucial factor

*Correspondence:
Krzysztof Kupczak
krzysztof.kupczak@us.edu.pl
[1] Institute of Earth Sciences, Faculty of Natural Sciences, University of Silesia in Katowice, Będzińska 60, 41-200 Sosnowiec, Poland
[2] Department of Metal Forming and Metallurgical Engineering, Faculty of Metals Engineering and Industrial Computer Science, AGH University of Krakow, Mickiewicza 30, 30-059 Cracow, Poland

enabling smelting, and so far, the best-described methods are those dedicated to temperature condition reconstructions. Phase diagrams, computer software, geothermometers, and high-temperature experiments allow determining both the liquidus and solidus temperatures of slags [5, 9, 11]. As both viscosity and oxidation–reduction conditions are temperature dependent, they cannot be accurately determined without the smelting temperature estimation [1, 4, 9, 10, 12].

Oxygen fugacity is one of the factors that should be considered in the reconstruction of metallurgical processes [1, 3, 10, 13, 14]. Knowledge about the fugacity of oxygen and sulfur allows to obtain a broad spectrum of information about the technological process and, indirectly, the society conducting it. The high fugacity of sulfur indicates the use of sulfide ores in the process or their addition, with the simultaneous lack of initial ore roasting. On the contrary, the low fugacity of sulfur indicates the use of oxide ores or preliminary roasting of sulfide ores. Combined with geological data from the area, this allows to drawn conclusions about the type of the ores used in the process and even the advancement of mining in the area. Commonly, in the case of sulfide ores, primary mineralization occurs deeper; thus, their exploitation may require an advanced process of excavation drainage, while oxide ores formed as a result of weathering of primary mineralization are closer to the surface [15]. The latter can often be exploited using the most straightforward techniques [16]. Naturally, the high fugacity of oxygen recorded in the slag indicates oxidizing conditions during the process, and low fugacity indicates reducing conditions. A significant variation in the fugacity of oxygen and sulfur within one sample may indicate a low homogeneity of the metallurgical process and its primitiveness [3, 10, 17, 18]. On the other hand, a considerable variation of oxygen and sulfur between different samples from the same location indicates a multistage metallurgical process [9, 19, 20].

Oxygen fugacity prevailing during historical metallurgical processes is most often determined by Fe buffers, which various authors have proposed [21, 22]. However, these methods have some limitations because they only consider the degree of iron oxidation in the analyzed slags [3, 9, 10, 17]. Although the redox conditions estimated with only the Fe buffers are generally correct, the oxygen fugacity prevailing during smelting can be determined more precisely by combining a few other elements occurring in slags. The widest possibilities in this field are provided by slags formed during the processing of nonferrous metal ores, especially polymetallic ores.

This study aims to present a new method for determining the fugacity of oxygen and sulfur during historical metallurgical processes based on predominance area diagrams (PAD). This method allowed determining the fugacity of oxygen and sulfur with much greater precision by considering the O_2 and S_2 fugacity-dependent phase reactions of many elements occurring in the slags. The additional goal was to combine obtained data with a wide range of experimental, geochemical, mineralogical, and petrographic methods to recreate the smelting conditions in the fifteenth to seventeenth century metallurgical processes in Polichno (Old Polish Industrial District, Holy Cross Mountains).

Location and historical/geological background

Polichno (Fig. 1) is a small village (less than 1000 inhabitants) located in the commune of Chęciny in the Świętokrzyskie voivodeship [23]. In Polichno, smelting activities processed the local copper ores since the fifteenth century [24]. The end of metallurgical production most likely came with the crisis of the Chęciny mining industry in the seventeenth century. From the eighteenth century, the resumption of metallurgical activities occurred in other locations in the Kielce region (e.g., Kielce, Wola Murowana) [24]. Historical sources do not contain data on smelting conditions. For this reason, provided information concerning the practical aspects of smelting is based on historical sources from that period [16]. In the vicinity of the analyzed area, copper (e.g., Miedzianka) and lead (e.g., Ołowianka; Fig. 1) deposits occur, and for this reason, the production in Polichno may have involved both metals [24]. Despite the type of metal produced, the first stage of the production process involved the crushing and enrichment of ores. The presence of a river near the smelter made it possible to use water power for this purpose. The ores were then sorted and smelted [16, 24]. At that time, during the lead production processes, the ores were roasted (oxidizing conditions) and then smelted with the addition of charcoal and fluxes (reducing conditions). During smelting, the lead flowed into the settler, from which it was then collected [10, 16, 24]. The production of copper from sulfide ores was carried out in two steps. In the first stage, speiss/matte was produced by heating the ore with charcoal with the addition of fluxes (reducing conditions). The speiss/matte was heated again (matte converting) with air blowing (oxidizing conditions). Additives (usually SiO_2) were added in this step to bond iron and other impurities within the slag melt, which was successively removed from the furnace. In this way, the semi-finished product was cleaned of Fe. The process was sustained until the sulfur/arsenic remaining in the furnace was oxidized and removed in gaseous form, leaving only the metallic copper [12, 25].

Considering that the Miedzianka deposit (Fig. 1) is the largest one exploited in the Polichno area, the

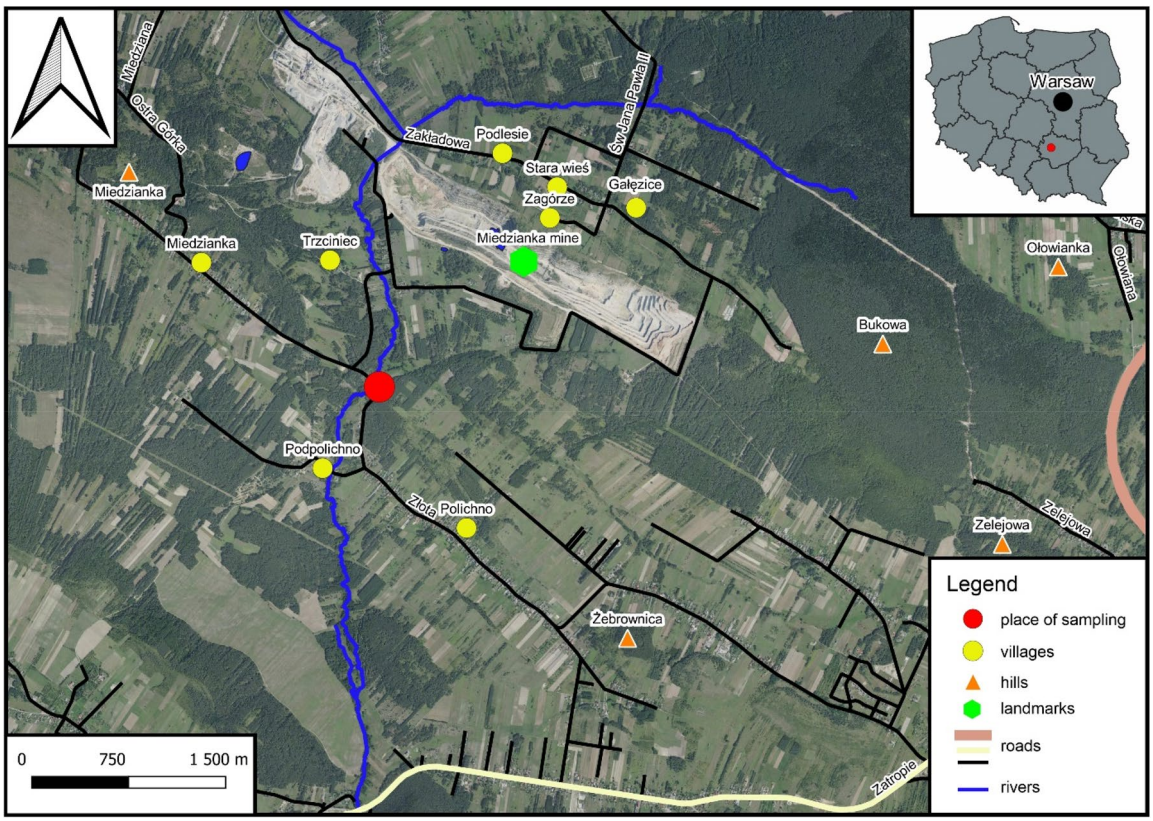

Fig. 1 Location map of the sampling site (made based on data from geoportal.gov.pl [26])

production was likely mainly based on it. Its exploitation since the fifteenth century is confirmed by mentions in a chronicle written by Jan Długosz in 1455–1480 [27]. The ore mineralization within the Miedzianka deposit is located in the southwestern part of the Holy Cross Mountains. Copper occurs both in the form of primary (sulfides, sulfosalts) and secondary mineralization (e.g., sulfides and carbonates) [28, 29]. Primary mineralization is associated with hydrothermal veins within carbonate rocks. The ore minerals mainly include tennantite ($(Cu,Fe)_{12}As_4S_{13}$), chalcopyrite ($CuFeS_2$), gersdorffite (NiAsS), bornite (Cu_5FeS_4), galena (PbS), and sphalerite (ZnS) [29]. The progressive weathering of carbonate rocks that host the primary minerals has resulted in forming zones enriched in secondary mineralization that mainly include chalcocite (Cu_2S), digenite (Cu_9S_5), covellite (CuS), bornite, malachite ($Cu_2(CO_3)(OH)_2$), azurite ($Cu_3(CO_3)_2(OH)_2$), chrysocolla ($(Cu,Al)_2H_2Si_2O_5(OH)_4 \cdot n(H_2O)$) [29]. Secondary mineralization occurs mainly within clays filling cracks in karsts [29]. In addition to copper and lead minerals, the presence of barite ($BaSO_4$) and hematite (Fe_2O_3) was observed in the Miedzianka [30].

Materials and methods

Sampling

Samples for analysis were collected in the Polichno village, on the road leading from Polichno to Miedzianka (Fig. 1). The slag dump was located in historical times. However, it was destroyed during the construction of the road [31], and now slags can only be found in scattered form in the soil profile. During the fieldwork, 48 slag samples ranging in size from 1 to 10 cm were collected from the soil profile 20 to 150 cm below the ground surface. Slag samples collected were divided into five main slag types (POL1–POL5; Fig. 2). The main criteria for the division were the macroscopic differences between the slags (color, crystallinity/glassiness of the samples). The slags were also divided according to the degree of weathering processes occurring on the samples and the homogeneity/heterogeneity of the slags. Representative material from each type of slag was taken for further analysis.

Chemical and phase analyzes

The collected slags were first subjected to microscopic observations. Several samples were made from each type

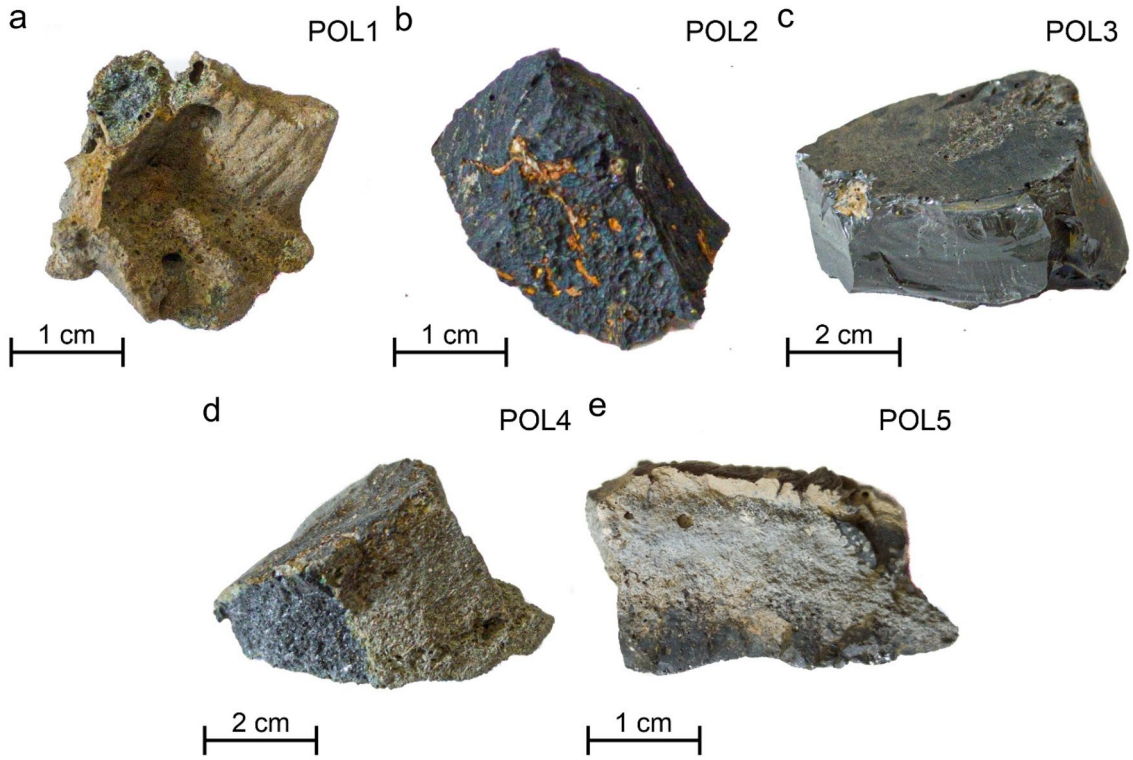

Fig. 2 Macroscopic photos of slags collected during fieldwork in Polichno

of slag for microscopic examination. An Olympus BX-51 polarizing microscope and a scanning electron microscope equipped with an energy dispersive spectrometer (SEM–EDS; Phenom XL) were used for this purpose (Institute of Earth Sciences, University of Silesia). Based on these observations, the slag texture was determined. EPMA (electron micro-probe microanalyzer) was used to determine the exact chemical composition of the phases present in the slags. A CAMECA SX100 electron microprobe (Inter-Institutional Laboratory of Microanalysis of Minerals and Synthetic Materials, University of Warsaw) was used for this purpose. The following standards were used during the EPM analyzes: Na—albite ($NaAlSi_3O_8$); Mg, Si, Ca—diopside ($[Ca,Mg,Fe]_2SiO_3$); Al, K—orthoclase ($KAlSi_3O_8$); Ba—barite ($BaSO_4$); Ti—rutile (TiO_2); Pb—crocoite ($PbCrO_4$); Fe—Fe_2O_3, chalcopyrite ($CuFeS_2$); Mn—rhodonite ($CaMn_3Mn[Si_5O_{15}]$); Zn—sphalerite (ZnS); P—YPO_4, $LaPO_4$; As—GaAs; Co—CoO; Ni—NiO; Cu—cuprite (Cu_2O); S—chalcopyrite ($CuFeS_2$), barite ($BaSO_4$); Sb—stibnite (Sb_2S_3). The slags were also analyzed for chemical composition using the combination of X-ray fluorescence (XRF) on fused discs and inductively coupled plasma emission/mass spectrometry (ICP-ES/ICP-MS). Samples representative of each type of slag were selected for bulk chemical composition analyses. The concentrations of P_2O_5, SiO_2 TiO_2, Al_2O_3, Fe_2O_3, MnO, CaO, MgO, Na_2O, K2O, SO_3, Ba, and LOI were determined by XRF. Concentrations of Cu, Pb, Zn, Ni, As, Sr, and Sb by ICP methods. During the ICP analyzes, multi-acid digestion was used. XRF and ICP-MS/ES analyses were performed by Bureau Veritas Mineral Laboratories (Canada). Loss of ignition was determined at 1000 °C.

High-temperature experiments

Slag samples were subjected to two high-temperature experiments to determine the slags' liquidus and solidus temperatures. In the first one, slag samples were grounded, formed into a cone with a diameter and height of 3 mm, and placed on a corundum plate. Then the plate was placed in the tube furnace and heated until the slag was completely liquefied with a temperature gradient of 70 °C/min to 900 °C, then 30 °C/min to 1100 °C/min, and 10 °C/min to 1350 °C. During heating, samples were observed using a high-temperature microscope (Leitz; Hesse Instruments; Faculty of Metals Engineering and Industrial Computer Science, Department of Metal Forming and Metallurgical Engineering, AGH University of Krakow; Cracow). During the observations, attention was paid to the first changes on the surface of the samples, indicating the start of melting (solidus temperature). Subsequently, the sphere, hemisphere, and flow

temperatures were distinguished. From the point of view of the conducted research, the most important is the flow temperature, which corresponds to the liquidus temperature. Flow temperature was determined when the height of the sample equaled 1/3 of the height of the sample at the hemisphere temperature [32].

Experimental smelting in a laboratory furnace was used as a second experimental method of slags' solidus and liquidus determinations. Two types of slags were selected for the experiment (POL2 and POL4), representing the two most diverse slags. The POL2 sample is the most common glassy type, and POL4 is the most commonly observed hypocrystalline slag. Slag fragments were then divided into several subsamples by crushing and cutting into fragments (about 1 cm^3). During the experiment, the samples were heated in crucibles for 3 h to a certain temperature (800 °C, 1000 °C, 1100 °C, 1150 °C, and 1200 °C). After reaching a certain temperature, the samples were kept at this temperature for 2 h. After this time, the samples were cooled with the temperature gradient of the furnace to ambient temperature. Each time after the experiment, the samples were removed from the furnace for examination, and a new subsample was taken for the next experiment. Experiments were performed at the high-temperature experiments laboratory at the Institute of Earth Sciences of the University of Silesia in the chamber furnace PLF 160/5 with a PC 442/18 controller, SiC heaters, and Thermocouple S with a maximum working temperature of 1550 °C.

Thermodynamic calculations

To determine the oxygen and sulfur fugacities, thermodynamic data [33] were used to construct predominance area diagrams (PADs) that accounted for the phase transitions between the most common phases observed in slags (metallic, oxides, and sulfides). The diagrams were created based on the method described by Barin [33] for the liquidus and solidus temperatures of the analyzed slags.

Results

Slags overview

In the samples from Polichno, hypocrystalline (POL1, POL4-5) and glassy slags (POL2-3) were distinguished (Fig. 2). Hypocrystalline samples had a gray color with pores up to 10 mm in diameter. The hypocrystalline slags' surface was characterized by a lighter color (layer up to 2 mm thick) compared to a darker color inside the slags (Fig. 2a, d). A lighter color was also observed around the pores. The color change suggests the progressive weathering of the slags. Glassy slags were most commonly black (POL2; Fig. 2b) or greenish (POL3; Fig. 2c) in color with small (about 1 mm) orange-colored layers (in POL2). This type of slag had a glassy luster in the cross-section and a dull luster on the surface (Fig. 2b, c), which resulted from the weathering process. Scattered quartz/cristobalite (SiO_2) crystals were observed within them during macroscopic observations. SiO_2 crystals were mainly in the form of small (less than 1 mm in diameter) crystals.

In POL1 slags, surface changes due to weathering are more evident than in other hypocrystalline samples (Fig. 2). Secondary crystallization in the form of a green surface (most likely malachite) is often observed on the surface of the samples. In the unaltered by weathering part of the slags, crystallization is visible in the form of very fine, barely visible phases. Microscopic observations of POL1 slags revealed the presence of phases from the wollastonite group ($CaSiO_3$; Fig. 3a; Table 1). Occasionally, calcite ($CaCO_3$) and single quartz/cristobalite crystals were also observed (Table 1). The presence of sulfides (mainly in the form of chalcocite), arsenides, and metallic Cu was also found (Table 1). Arsenides (domeykite (Cu_3As) and CuFeAs) were slightly less common than sulfides. Sulfide and arsenide phases most often co-occur as oval phases (up to 30 μm). Still, larger aggregations were also observed (Fig. 3a). Metallic copper was found only in areas with higher Cu sulfide/arsenide concentrations (Fig. 3a; Table 1).

During microscopic observations, it was confirmed that POL2 slags were mainly composed of glassy phases. PbO-enriched glasses were observed among other glassy phases as bright (in BSE imaging) domains (Fig. 3b). Crystals of quartz/cristobalite, pyroxene (usually up to several μm in length), and oval phases (up to 50 μm in diameter) containing mainly litharge and sometimes galena (up to 20 μm in diameter) were scattered within the glass (Fig. 3b; Table 1). Occasionally the oval metallic phases composed of metallic Cu and Pb (up to 15 μm in diameter) were observed (Table 1). Barite and cerussite ($PbCO_3$) were also found within these slags (Table 1), mainly in the form of aggregates up to 100 μm in length.

In POL3 slags, only dispersed metallic phases and pyroxene were observed within the glass. Metallic phases were mainly composed of metallic Cu and Fe (Fig. 3c; Table 1). Sometimes, metallic Cu coexisted with copper sulfides and arsenides. The diameter of metallic phases reached up to 600 μm (Fig. 3c). While metallic Cu was commonly found within POL3 slags, metallic Fe was observed only sporadically.

POL4 slags were hypocrystalline (Fig. 2d; Fig. 3d), and the changes resulting from weathering are not as advanced as in POL1 slags. On the surface of these samples, secondary crystallization was not observed as far-reaching as in POL1 slags. The slag's inner part is dark gray with clearly visible crystalline phases

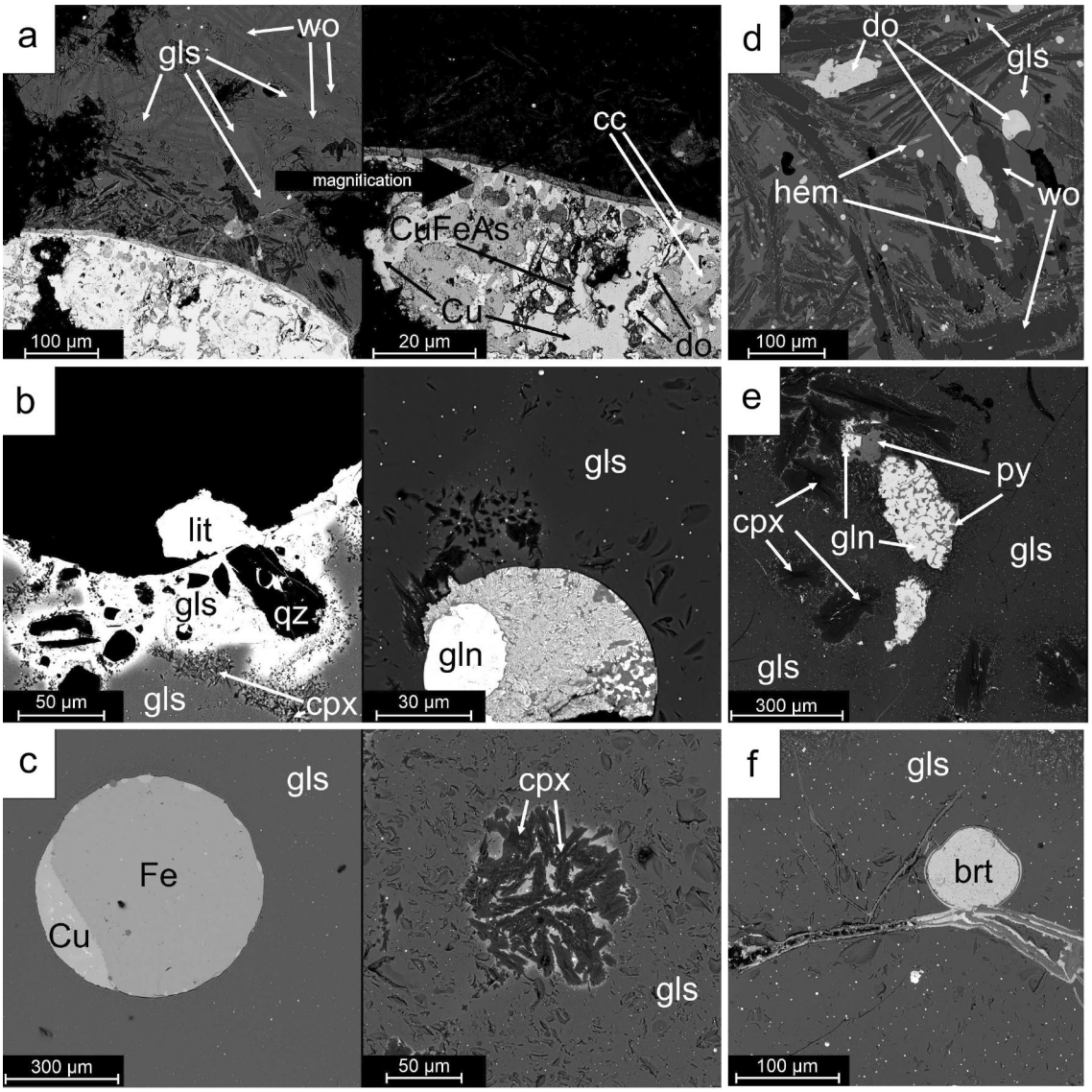

Fig. 3 Representative BSE images of the analyzed slags: **a** POL1; **b** POL2; **c** POL3; **d** POL4; **e**, **f** POL5. brt—barite; cc—chalcocite; Cu—metallic copper; cpx—clinopyroxene; do—domeykite; Fe—metallic iron; gln—galena; gls—glass; hem—hematite; lit—litharge; py—pyrrhotite; wo—wollastonite; qz—quartz

Table 1 Phases occurring in slags from Polichno

	POL1	POL2	POL3	POL4	POL5
Silicates	Wollastonite	Pyroxene	Pyroxene	Wollastonite	Pyroxene
Oxides	SiO_2 phases	SiO_2 phases, Litharge	SiO_2 phases	Hematite	SiO_2 phases, Litharge
Metallic phases	Cu	Cu, Pb	Cu, Fe	Cu	–
Sulfides	Chalcocite	Galena	Chalcocite	Chalcocite	Galena, Pyrrhotite
Arsenides	Domeykite, CuFeAs	–	Domeykite	Domeykite	–
Sulfates	–	Barite	–	–	Barite
carbonates	–	Cerussite	–	Calcite	–

that reach up to 2 mm in length. During microscopic observations, it was found that the main phase present in the slags was skeletal wollastonite. The wollastonite crystals are up to several hundred μm in length and were dispersed within the glassy material (Fig. 3d; Table 1). Hematite crystals up to a dozen μm long (Fig. 3d), calcite, and oval phases containing copper were also scattered in the glass (Fig. 3d; Table 1). These phases had a diameter of up to 100 μm and were mainly composed of arsenides, sulfides, and metallic Cu (Fig. 3d; Table 1).

POL5 slags are the least homogeneous of all slag types. The inner part of the slags is light gray (Fig. 2). The crystalline phases are mostly very small and barely visible. However, larger crystals can occasionally be seen, reaching several mm in length. Within the POL5 slags, zones of darker color can also be seen (Fig. 2). During microscopic observations, quartz/cristobalite (up to 150 μm in length), skeletal pyroxene up to 200 μm long, and oval clusters containing litharge (PbO), galena (PbS), and pyrrhotite ($Fe_{1-x}S$) were observed (Fig. 3e; Table 1). In the POL5 slags, oval barite crystals up to 90 μm in diameter were also observed (Fig. 3f; Table 1).

Slags composition and chemistry of phases

The POL1–POL5 slags were mainly composed of SiO_2 (34.88–49.69 wt.%), FeO (12.62–17.71 wt.%), CaO (12.57–29.95 wt.%), and to a lesser extent of Al_2O_3 (up to 4.32 wt.%), P_2O_5 (up to 2.95 wt.%), and MgO (up to 1.01 wt.%; Table 2). The presence of Cu (up to 27,746 ppm) and Pb (up to 39,941 ppm) was also found in Polichno slags (Table 2). In one of the samples (POL2), increased content of BaO (24.48 wt.%) and Sr (up to 3748 ppm) was distinguished. Compared to POL1 and POL4-5 in POL2-3 slags, higher content of SiO_2 (up to 49.69 wt.%), Pb (18,954–39,941 ppm) with a reduced CaO content (up to 19.20 wt.%; Table 2) was observed. In POL1, POL4-5 slags, an increased concentration of Cu (16,918–27,746 ppm), As (up to 9166 ppm), and Sb (up to 1391 ppm) was observed (Table 2).

Silicates

In Polichno slags, silicates occurred as wollastonite in POL1 and POL4 samples and as clinopyroxene in POL2-3 and POL5 samples (Fig. 3). Wollastonite crystals were characterized by the substitution of Fe (0.15–2.3 wt.% of FeO), and less than 0.50 wt.% of oxide of Ti, Al, Mg, Mn, and Zn. Clinopyroxene crystals had a chemical composition corresponding to a diopside-hedenbergite

Table 2 Bulk chemical composition of slags from Polichno

		POL1	POL2	POL3	POL4	POL5
P_2O_5	wt.%	2.95	2.14	2.13	2.90	2.66
SiO_2		36.64	38.02	49.69	34.88	37.77
TiO_2		0.26	0.18	0.23	0.20	0.21
Al_2O_3		4.32	2.82	3.80	3.42	3.64
FeO		17.71	12.62	17.61	15.90	17.64
MnO		0.63	0.63	0.41	0.43	0.72
CaO		25.49	12.57	19.20	29.95	27.50
MgO		0.52	1.01	0.64	0.44	0.56
BaO		0.69	24.48	0.77	0.90	1.61
Na_2O		0.23	0.05	0.23	0.23	0.19
K_2O		0.97	0.72	1.19	0.81	0.87
SO_3		0.06	0.90	0.35	0.03	0.19
TOT/C		0.30	0.02	0.02	0.09	0.15
TOT/S		0.02	0.48	0.15	< 0.02	0.10
LOI		− 0.9	− 2.0	− 2.2	− 1.4	− 0.8
Cu	ppm	27,746	415	11,054	22,853	16,918
Pb		7104	39,941	18,954	7773	11,496
Zn		20,427	22,225	6921	31,970	15,464
Ni		150	11	164	368	121
As		6248	220	814	9166	5963
Sb		1142	38	387	1391	719
Sr		282	3748	407	298	508

TOT/C—total carbon; TOT/S—total sulfur; LOI—Loss on ignition

Table 3 Representative EPMA analyses of silicates, oxides, carbonates, and average composition of glassy phases occurring in Polichno slags

	wo POL4	**wo POL4**	**cpx POL5**	**qz POL2**	**hem POL4**	**hem POL4**	**cal POL4**	**cer POL2**	**gls1 (n = 4) POL1**	**gls2 (n = 6) POL2**	**gls3 (n = 4) POL3**	**gls4 (n = 5) POL4**	**gls5 (n = 4) POL5**
P_2O_5	na	na	na	bdl	na	na	0.50	0.19	4.4	1.85	2.1	3.7	3.0
SiO_2	50.2	51.7	48.3	99.4	0.49	0.63	bdl	bdl	47.9	41.3	51.7	34.4	40.0
TiO_2	0.08	bdl	bdl	bdl	0.41	0.45	na	bdl	0.36	0.25	0.21	0.14	0.28
Al_2O_3	0.29	bdl	0.27	bdl	2.3	2.1	bdl	bdl	6.0	3.8	4.1	4.0	3.5
FeO^{calc}	2.3	0.15	20.4	bdl	–	–	bdl	bdl	8.5	22.8	16.5	11.9	24.7
$Fe_2O_3^{calc}$	–	–	–	–	88.8	89.6	–	–	–	–	–	–	–
MnO	0.30	bdl	2.1	bdl	0.45	0.51	bdl	bdl	0.36	1.10	0.36	0.45	1.15
CaO	45.6	48.8	25.7	bdl	0.69	0.68	53.3	bdl	27.7	11.5	19.6	31.0	14.88
MgO	0.21	bdl	1.79	bdl	0.37	0.33	bdl	bdl	0.61	0.75	0.65	0.65	0.74
ZnO	0.34	bdl	0.31	bdl	6.2	5.2	bdl	bdl	0.32	0.50	0.59	7.1	0.99
CuO	bdl	bdl	bdl	bdl	na	na	na	bdl	0.24	0.00	0.15	0.21	0.00
PbO	bdl	bdl	bdl	bdl	na	na	bdl	83.4	0.03	6.4	0.67	0.75	3.75
Na_2O	bdl	bdl	bdl	bdl	0.17	bdl	bdl	bdl	0.21	0.14	0.18	0.51	0.30
K_2O	bdl	bdl	bdl	bdl	bdl	bdl	bdl	bdl	1.37	0.87	1.35	0.97	0.86
NiO	bdl	bdl	bdl	na	0.58	0.51	na	bdl	na	na	na	na	na
BaO	na	na	na	bdl	na	na	na	0.32	0.77	7.1	0.41	0.90	5.33
As_2O_3	bdl	bdl	bdl	bdl	na	na	na	bdl	0.07	0.00	0.00	1.81	0.00
SO_3^{calc}	na	na	na	bdl	na	na	na	bdl	0.00	0.28	0.00	0.00	0.59
SO_2^{calc}	na	na	–	na	na	na	0.21	–	–	–	–	–	–
CO_2^{calc}	na	na	–	–	–	–	46.0	16.28	–	–	–	–	–
Total	99.32	100.65	98.87	99.40	100.46	100.01	100.01	100.19	98.84	98.64	98.57	98.49	100.07
	a.p.f.u												
P	–	–	–	–	–	–	0.01	–					
Si	0.99	1.00	1.98	1.00	0.01	0.02	–	–					
Ti	–	–	0.00	0.00	0.01	0.01	–	–					
Al	0.01	–	0.01	0.00	0.07	0.07	–	–					
Fe^{2+}	0.04	–	0.70	0.00	0.00	0.00	–	–					
Fe^{3+}	–	–	–	–	1.78	1.80	–	–					
Mn	–	–	0.07	–	0.01	0.01	–	–					
Ca	0.96	1.01	1.13	–	0.02	0.02	0.93	–					
Mg	0.01	–	0.11	–	0.01	0.01	–	–					
Zn	–	–	0.01	–	0.12	0.10	–	–					
Cu	–	-	–	–	–	–	–	–					
Pb	–	–	–	–	–	–	–	1.03					
Na	–	–	–	–	0.01	–	–	–					
K	–	–	–	–	–	–	–	–					
Ni	–	–	–	–	0.01	0.01	–	–					
Ba	–	–	–	–	–	–	–	–					
As^{3+}	–	–	–	–	–	–	–	–					
S^{6+}	–	–	–	–	–	–	–	–					
S^{4+}	–	–	–	–	–	–	0.01	–					
C	–	–	–	–	–	–	1.02	0.99					
Total	2.00	2.00	4.01	1.00	2.06	2.04	0.94	2.01					
O^{2-}	3.00	3.00	6.00	2.00	3.00	3.00	3.00	3.00					

cal—calcite; cer—cerussite; cpx—clinopyroxene; gls—glass; hem—hematite; lit—litharge; wo—wollastonite; qz—quartz

solid solution and were composed of Si (up to 48.3 wt.% of SiO_2), Fe (up to 20.4 wt.% of FeO), Ca (up to 25.7 wt.% of CaO), and Mg (up to 1.79 wt.% of MgO), with Mn (up to 2.1 wt.% of MnO), Zn (up to 0.31 wt.% of ZnO), and Al (up to 0.27 wt.% of Al_2O_3) substitutions (Table 3).

Oxides

Oxides in the slags from Polichno occur in the form of hematite. Hematite crystals (88.8–89.6 wt.% of Fe_2O_3) were frequently observed in POL4 slags (Fig. 3d). In hematite, the substitution of Zn (5.2–6.2 wt.% of ZnO), Al (2.1–2.3 wt.% of Al_2O_3), and in a smaller amount (less than 1.00 wt.% of oxide) of Ti, Si, Mn, Ca, Mg, Ni, and Na were commonly observed (Table 3).

Glass

The glass was present in all types of slags, differing in chemical composition. In POL1–POL5 glass mainly consists of SiO_2 (34.4–51.7 wt.%), CaO (11.5–31.0 wt.%), and FeO (8.5–24.7 wt.%), with smaller content of ZnO (0.32–7.1 wt.%), P_2O_5 (1.85–4.4 wt.%), Al_2O_3 (3.5–6.0 wt.%), As_2O_3 (up to 1.81 wt.%), BaO (up to 7.1 wt.%), and K_2O (up to 1.37 wt.%; Table 3). The remaining elements were in amounts less than 1 wt.% of oxide (Table 3).

Carbonates

Carbonates were represented by cerussite (Table 3). In cerussite, the substitutions of Ba (up to 0.32 wt.% of BaO) and P (up to 0.19 wt.% of P_2O_5) were observed (Table 3). Cerussite was most likely formed during the weathering of slags.

Sulfides, arsenides, and metallic phases

Sulfides in the analyzed slags occurred as chalcocite, pyrrhotite, and galena. In chalcocite, substitutions of Fe (up to 0.60 wt.%), As (up to 0.43 wt.%), Pb (up to 0.42 wt.%), and less than 0.2 wt.% of Al, P, Si, Ca were observed (Table 4). In galena, less than 0.30 wt.% of Fe and Cu were

Table 4 Representative EPMA analyses of sulfides, arsenides, and metallic phases occurring in Polichno slags

	gln	pyh	cc	do	do	CuFeAs	Metallic phases				
	POL5	POL5	POL3	POL4	POL3	POL1	POL3	POL3	POL3	POL4	POL3
S	13.4	36.2	19.7	0.15	0.10	0.11	0.11	bdl	0.06	bdl	bdl
Fe	0.23	62.4	0.60	0.27	0.38	36.1	82.3	90.9	bdl	0.18	1.04
Co	bdl	bdl	bdl	bdl	bdl	0.65	0.82	0.91	bdl	bdl	bdl
Ni	bdl	bdl	bdl	0.36	1.55	1.07	0.63	0.35	1.21	0.37	bdl
Cu	0.29	0.86	77.8	70.0	66.7	23.2	1.69	2.3	76.4	81.9	94.0
As	bdl	bdl	0.43	28.1	23.0	37.5	2.9	2.5	18.0	17.4	1.17
Al	bdl	bdl	0.12	bdl	bdl	bdl	bdl	bdl	bdl	bdl	0.18
Sb	bdl	bdl	bdl	0.78	9.0	bdl	0.13	bdl	5.6	0.94	1.91
Pb	86.9	bdl	0.42	bdl	bdl	bdl	bdl	bdl	bdl	0.15	bdl
P	bdl	bdl	0.07	bdl	0.09	0.35	11.0	2.1	0.10	bdl	0.41
Si	bdl	bdl	0.09	bdl	bdl	bdl	bdl	bdl	bdl	bdl	0.10
Ca	bdl	bdl	0.09	bdl	bdl	bdl	bdl	bdl	bdl	bdl	bdl
Total	100.82	99.46	99.32	99.66	100.82	98.98	99.58	99.06	101.37	100.94	98.81
	a.p.f.u						Atomic concentration				
S	1.00	1.00	1.00	0.01	0.01	0.01	–	–	0.12	–	–
Fe	–	0.99	0.02	0.01	0.02	1.29	1.87	91.17	0.00	0.21	1.62
Co	–	–	–	–	–	0.02	–	0.87	–	–	–
Ni	–	–	–	0.02	0.07	0.04	–	0.33	1.36	0.41	–
Cu	–	0.01	2.00	2.94	2.86	0.73	93.76	2.00	79.39	83.74	96.31
As	–	–	0.01	1.00	0.84	1.00	4.03	1.84	15.87	15.09	0.87
Al	–	–	0.01	–	–	–	0.23	–	–	–	0.25
Sb	–	–	–	0.02	0.20	–	0.12	–	3.03	0.50	0.76
Pb	0.98	–	–	–	–	–	–	–	–	0.05	0.05
P	–	–	–	0.00	0.01	0.02	–	3.80	0.22	–	–
Si	–	–	–	–	–	–	–	–	–	–	0.15
Ca	–	–	–	–	–	–	–	–	–	–	–
Total	1.98	2.00	3.03	4.00	4.00	3.11	100.00	100.00	100.00	100.00	100.00

cc—chalcocite; do—domeykite; gln—galena; py—pyrrhotite

observed (Table 4). In pyrrhotite Cu (up to 0.86 wt.%; Table 4) substitution was found. Arsenide phases were represented by domeykite and CuFeAs. In domeykite, the substitutions of Sb (0.78–9.0 wt.%), Ni (0.36–1.55 wt.%), and less than 0.5 wt.% of Fe, S, and P were found (Table 4). Due to the amphoteric character of Sb, part of it (in domeykites) was calculated as a cation and part as an anion to balance the unit cell. In CuFeAs phases, substitutions of Ni (up to 1.07 wt.%) and less than 1 wt. % of Co, P, and S were observed (Table 4). Two types of metallic phases were observed in the analyzed slags. The most common metallic Cu was composed of 76.4–94.0 wt.% Cu, 1.17–18.0 wt.% As, 0.94–5.6 wt.% Sb, up to 1.21 wt.% Ni, up to 1.04 wt.% Fe, and smaller amounts (< 1 wt.%) of S, Al, Pb, P, Si (Table 4). The second type was metallic Fe. It was mainly composed of Fe (82.3–90.9 wt.%), P (2.1–11.0 wt.%), As (2.5–2.9 wt.%), Cu (1.69–2.3 wt.%), Co (0.82–0.91 wt.%), Ni (0.35–0.63 wt.%), S (up to 0.11 wt.%), and Sb (up to 0.13 wt.%; Table 4).

Restitic phases

Restitic phases in the analyzed slags are observed in the form of quartz, calcite, and barite. They are most likely residues from additives added during smelting and were not melted/decomposed during smelting. Quartz crystals consist only of SiO_2 (99.4 wt.%; Table 3). No substitutions have been found in their crystal structure (Table 3). In calcite, substitutions of P (up to 0.50 wt.% of P_2O_5) and S (up to 0.21 wt.% of SO_2) were observed (Table 3).

Temperature

Phase diagrams were one of the methods used to determine the slags' liquidus temperature. Calculations were based on the slags' total chemical composition and the glasses' averaged chemical composition. Considering that slags consist mainly of SiO_2, CaO, and FeO (63.21–86.50 wt.%) SiO_2-CaO-FeO diagram [34] is the best fit, although taking into account the presence of Al_2O_3 (2.82–4.32 wt.%) SiO_2-CaO-FeO-6% Al_2O_3 diagram was also used [35] (Fig. 4). The temperature of slags determined with SiO_2-CaO-FeO diagram was in the range of 1200–1600 °C (Fig. 4; Table 5). Based on the SiO_2-CaO-FeO-6% Al_2O_3 diagram, the liquidus temperature ranged from 1060 to 1350 °C (Fig. 4; Table 5).

The second method used during temperature determinations was the high-temperature microscope observations. The first deformations during the heating of the samples appeared at temperatures in the range of 821 °C (POL2)-1100 °C (POL1) (Additional file 1). The edges of the cone became rounded, indicating that the slag's solidus temperature was exceeded. The liquefaction of the slags was observed at the temperature range of 1126 °C (POL2) to 1263 °C (POL1). At this point, the samples reached flow temperature (Table 5; Additional file 1).

The next method of temperature determination was the high-temperature experiments. The first changes on the surface of the sample in the form of rounding the edges of POL2 slags appeared at 800 °C (Fig. 5; Table 5). In the case of sample POL4, the changes were evident when the sample was heated to 1100 °C (Fig. 5). The rounding of the edges indicates that the solidus temperature has been exceeded. Further changes during the experiments appeared when sample POL2 was heated to 1100 °C and sample POL4 to 1200 °C (Fig. 5). At these temperatures, sample POL4 melted completely, while sample POL2 melted almost entirely, but the quartz grains remained

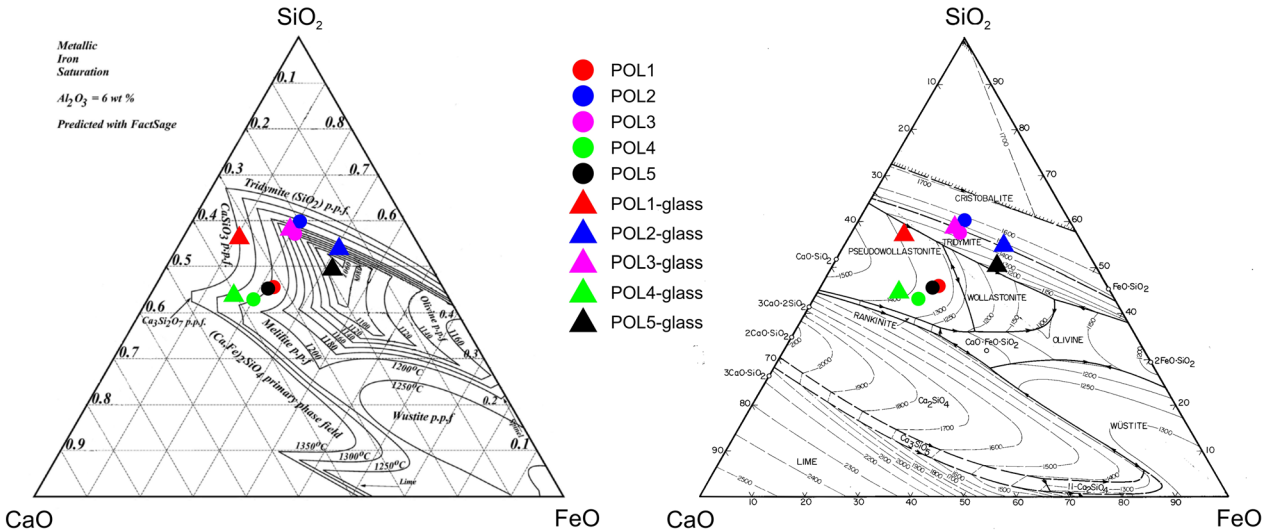

Fig. 4 Phase diagrams with the marked chemical composition of slags from Polichno [34, 35]

Table 5 Summary of temperatures determined during the analysis of slags with various methods

	Temperature in °C	POL1	POL2	POL3	POL4	POL5
Experiment	Liquidus	–	1100 (for glass) 1200 (including SiO_2 grains)	–	1200	–
	Solidus		800		1100	
Microscope observations	Liquidus	1263	1126	1154	1138	1246
	Solidus	1100	821	1090	1060	1058
CaO-SiO_2-FeO diagram	Bulk composition	1300–1400	1500–1600	1400–1500	1300–1400	1300–1400
	Glass	1300–1400	1400–1500	1400–1500	1400–1500	1200–1300
CaO-SiO_2-FeO-6% Al_2O_3 diagram	Bulk composition	1200–1250	1250–1300	1120–1160	~1250	~1250
	Glass	1300–1350	1140–1180	1160–1180	1250–1300	1060–1080

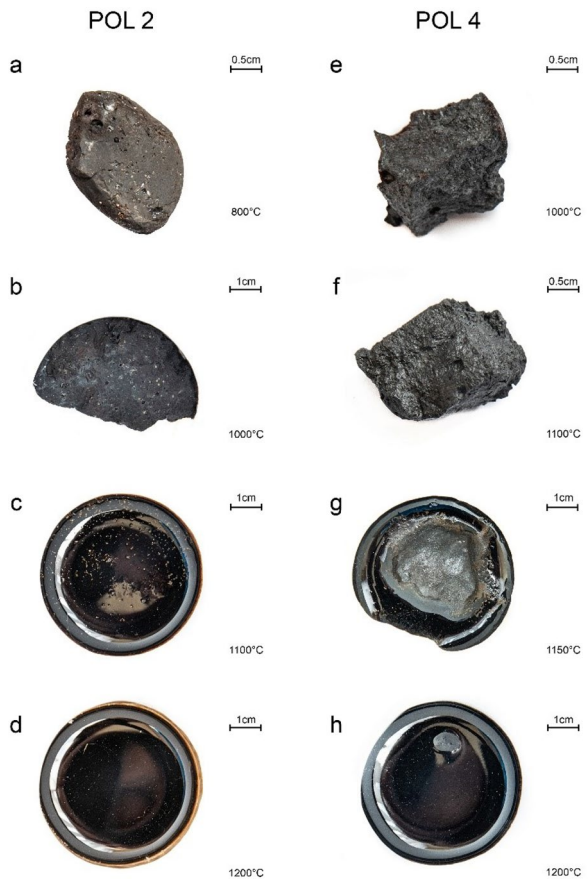

Fig. 5 Macroscopic photos of slags after the high-temperature experiments

unmelted (Fig. 5). Melting of the entire volume (including quartz grains) was observed when the sample POL2 was heated to 1200 °C (Fig. 5). Considering that the unmelted SiO_2 crystals occur in samples of glassy slag, the POL2 slag must result from smelting at a temperature close to 1100 °C and definitely below 1200 °C (Fig. 5; Table 5). Taking into account the similarity in the chemical composition of POL1, POL4-5 slags, the temperatures obtained from the experiment for sample POL4 are also reliable for samples POL1 and POL5.

The volatile properties during smelting

Analyses of the oxygen and sulfur fugacities during the smelting process in the Polichno were based on the thermodynamic data available in the literature [33]. As these data are available only for the temperature interval of 100 K, logK and temperature were plotted on the graph (Additional file 2). Then, the value of the logK for the desired temperature (liquidus and solidus of slags) was read from the graph (Additional file 3). The values were used to calculate the oxygen and sulfur fugacities under which the coexistence of sulfides (MeS), oxides (MeO), and metallic phases (Me) is possible (Additional file 3).

Calculating equilibrium constants (Additional file 3) made it possible to create the predominance area diagrams (Fig. 6). Then, based on the slags' phase composition, the oxygen and sulfur fugacities during the formation of individual types of slags were determined. The line showing the equilibrium constant between the metallic and oxide/sulfide phases shows the conditions under which the coexistence of metallic and sulfide/oxide phases is possible. It also provides information on the minimum sulfur/oxygen fugacity in which the formation of sulfides/oxides is possible.

Considering that in the POL1 slags, Cu occurs mainly in the metallic form or as the sulfides/arsenides, the $\log P_{O_2}$ during their formation had to be below −5.16 at the solidus temperature (1100 °C) and below −4.30 atm. at the liquidus temperature (1200 °C; Fig. 6; Table 1; Additional file 3). The coexistence of metallic Cu and Cu sulfides in slags is possible at the sulfur fugacity ($\log P_{S_2}$) in the range of −6.59 (in 1100 °C) and −5.84 atm. at 1200 °C (Fig. 6; Additional file 3).

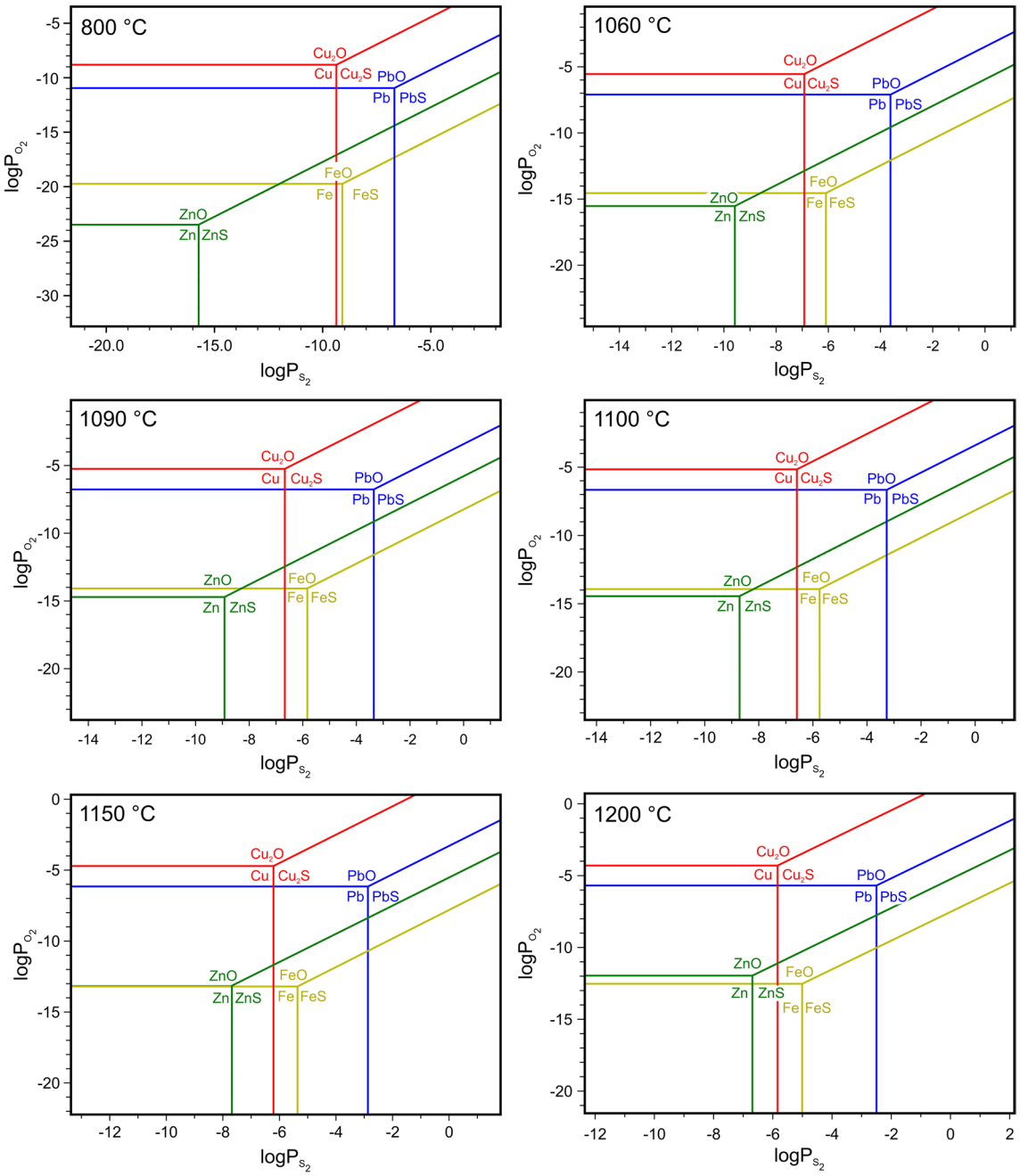

Fig. 6 Predominance area diagrams considering the most important metals present in slags after copper production

In POL2 slags, lead occurs mainly in glassy phases (as PbO) and as litharge. The oxygen fugacity under which Pb was oxidized for liquidus and solidus temperatures should be higher than $\log P_{O_2} = -10.95$ (at 800 °C) and -6.66 (at 1100 °C; Fig. 6; Additional file 3). Under conditions close to thermodynamic equilibrium between PbO and metallic Pb, it was also possible for metallic Pb to occur, which was occasionally observed in POL2 slags (Table 1). Occasionally observed metallic Cu indicates the $\log P_{O_2}$ lower than -8.81 at 800 °C and -5.16 at 1100 °C. The presence of sulfide phases only in the form of PbS indicates the sulfur fugacity above $\log P_{S_2} = -6.68$ at 800 °C and above -3.28 atm. at 1100 °C (Fig. 6; Additional file 3).

Due to the lack of copper oxides in POL3 slags, the oxygen fugacity during their formation had to be lower

than $\log P_{O_2} = -5.25$ (at 1090 °C) and −5.16 atm. (at 1100 °C; Fig. 6; Additional file 3). In POL3 slags, metallic Fe was found (Fig. 3c), but its presence is an exception in the scale of the analyzed material. At the same time, metallic Fe occurs surrounded by a glass containing oxidized Fe (Fig. 3c; Table 3). Considering the presence of Fe in the metallic and oxide form, the oxygen fugacity in these zones ranges from $\log P_{O_2} = -14.08$ (1090 °C) to −13.93 atm. (1100 °C; Fig. 6; Additional file 3). The coexistence of metallic Cu with Cu sulfides indicates the local thermodynamic equilibrium between Cu_2S and metallic Cu (Fig. 3a). It is possible in the range of sulfur fugacity between $\log P_{S_2} = -6.67$ at 1090 °C and −6.59 atm. at 1100 °C (Fig. 6; Additional file 3). The absence of Fe sulfides confirms sulfur fugacity below $\log P_{S_2} = -5.83$ (at 1090 °C) and −5.75 atm. (at 1100 °C; Fig. 6; Additional file 3).

In POL4 slags, no copper oxides were found, which proves the $\log P_{O_2}$ was below −5.55 at the solidus temperature (1060 °C) and below −4.30 atm. at the liquidus temperature (1200 °C; Fig. 6; Additional file 3). Occasionally observed Cu sulfides and the absence of Fe sulfides indicate sulfur fugacity in the range of $\log P_{S_2} = -6.92$ to −6.09 atm. (at 1060 °C) and −5.84 to −5.01 atm. (at 1200 °C; Fig. 6; Additional file 3).

The presence of Pb in the oxidized form in POL5 slags was possible with the minimum oxygen fugacity of $\log P_{O_2} = -7.10$ (at 1060 °C) and −5.69 atm. (at 1200 °C; Fig. 6; Additional file 3). Iron sulfides' presence indicates the minimum sulfur fugacity of $\log P_{S_2} = -6.09$ at 1060 °C and −5.01 atm. at 1200 °C (Fig. 6). The presence of Pb sulfides proves greater sulfur availability (at least $\log P_{S_2} = -3.62$ at 1060 °C and −2.50 atm. at 1200 °C; Fig. 6; Additional file 3).

Discussion

Recreation of the copper smelting process at Polichno

The temperature range at which copper smelting was carried out is crucial to determine the oxygen and sulfur fugacities during the metallurgical process. In this study, we decided to use three independent methods of smelting temperature determination. High-temperature experiments and observations using a high-temperature microscope made it possible to determine the liquidus (1100–1200 °C) and solidus (800–1100 °C) temperatures of the analyzed slags. Temperatures determined by high-temperature microscope observations differ from those determined by experimental smelting.

In the case of glassy slags (POL2), the temperatures determined by microscope observations are higher than those obtained from experiment in a laboratory furnace. The differences are only 21–26 °C for solidus and liquidus temperatures, respectively (Table 5). These differences are most likely due to the rate at which the samples were heated. Regardless of the target temperature, the sample was heated for 3 h during heating in the laboratory furnace. Then, a high temperature was maintained for 2 h. In contrast, during microscopic observations, the temperature gradient ranged from 10 °C (0–900 °C) to 70 °C (1100–1350 °C) per minute. With a rapid temperature change, changes on the surface of the samples could be observed with a delay.

In the POL4 sample, the temperatures determined with the microscope were lower than that determined during experimental smelting. The sample was heated from ambient temperature until complete liquefaction during microscopic observations. For practical reasons, experimental smelting is carried out with only a temperature interval of 50–100 °C, limiting the possibility to observe changes in temperature between this range. A lower liquidus temperature determined during microscopic observations is because the liquidus temperature was considered the one at which the sample liquefied enough to reach the flow temperature (1138 °C; Table 5). As the experiments in the laboratory furnace showed the POL4 sample at 1150 °C was liquid enough to spread to the bottom of the crucible (Fig. 5). However, the sample did not homogenize, which indicates the presence of solid phases within the sample.

Considering the above it was decided to base further considerations on the liquidus temperature determined by high-temperature experiments in a laboratory furnace. In the case of solidus temperature, the first signs of melting are essential. For this reason, the lowest temperature obtained during the experiments should be considered the solidus temperature.

The use of experimental smelting and the presence of unmelted phases in glassy slags made it possible to determine the maximum smelting temperature for glassy (POL2) slags at 1200 °C. At this temperature, all previously unmelted fragments were melted (Additional file 3). It was impossible to determine the maximum smelting temperature for hypocrystalline slags due to the lack of unmelted phases in the slags. The high-temperature experiments allowed the verification of temperature estimations obtained from the phase diagrams. The best diagram was the SiO_2-CaO-FeO-6% Al_2O_3 phase diagram due to the broadest spectrum of the elements included. Its accuracy of the determined temperature is also positively affected by the diagram design with a marked temperature interval of 20 °C (Fig. 4; Table 5).

The smelting temperature of the Polichno slags is slightly lower than observed in other locations where copper smelting was carried out in historical times, e.g., in Marsiliana (1150–1300 °C) [18], Rudawy Janowickie (1200–1300 °C) [6], and in Kondratów and Leszczyna

(1210–1400 °C) [3]. It is also worth noting that glassy slags' first signs of melting appear as early as 800 °C (Fig. 5; Table 5). Such low temperatures are rare and have so far only been described in a few places [4, 36]. Of the slags analyzed, only POL2 had such a low solidus temperature. This type of slag is distinguished from the others by its high content of Pb, Zn, and BaO (Table 2). Taking into account that POL2 are glassy slags (Figs. 2, 3), these elements are mainly included in the amorphous phases (in oxide form; Table 3) generating low solidus temperatures (Table 5). Moreover, due to the presence of unmelted SiO_2 grains within slags, it was possible to determine the maximum temperature at which glassy slags formed. During experiments, the complete meltdown of SiO_2 grains indicated that the smelting temperature must have been lower than 1200 °C. So far, only the minimum smelting temperature has been determined in the reconstruction of historical metallurgical processes [3–5, 9, 10, 18].

Accurate determination of temperature conditions made it possible to determine the fugacity of gases during smelting. The fugacity of O_2 and S_2 was determined with the PADs constructed based on thermodynamic calculations. The conducted research showed a relatively large range ($\log P_{O_2}$ from −4.30 at 1200 °C to −19.93 at 1100 °C) of oxygen fugacity in which the production process in Polichno could have been carried out. In the studies conducted so far, oxygen fugacity was often determined in a narrower range [1, 14, 17]. However, the greater accuracy comes from determining oxygen fugacity in these cases for only one temperature [1, 14] or a narrower temperature range [17]. The broad range of values presented in this study is due to various slag types and a wide range of considered smelting temperatures. When determining the redox conditions for particular slag types, oxygen fugacity was often determined over a much narrower range. The type of metal produced is also not insignificant. In the case of slags after Fe production [14, 17], it was necessary to maintain a more reductive environment during smelting. Because of this, the range of oxygen fugacity in which production could have been carried out was narrower and had to be close to the value at which Fe is reduced to metallic form. In the case of Cu production, it was not necessary to maintain a highly reducing environment. Still, values close to the equilibrium line between FeO and Fe were obtained during the process in Polichno in some zones, by which metallic Fe is observed in the slags (Fig. 3c).

The range of oxygen fugacity in which smelting was carried out in Polichno is slightly lower compared to the conditions prevailing in smelters operating during a similar period in Marsiliana, Kondratów, and Leszczyna (Table 6). The difference is mainly due to the lower temperatures prevailing during smelting in Polichno. For the oxide/sulfide phases to be reduced at lower temperatures, it is necessary to maintain a more reducing environment (Fig. 6). In one of the oldest copper smelters (3rd millennium BC in Cabrières and Bronze Age in Crete), the range of oxygen fugacity in which smelting was carried out is comparable to that prevailing during smelting at Polichno (Table 6). Whenever $\log P_{O_2}$ values are lower, it indicates a more reductive environment, which may have been achieved by using more reductant (charcoal) during smelting.

Because there is no information on the addition of sulfur during the copper production process in historical times, the fugacity of sulfur depends on the amount of sulfide minerals occurring in the ore. Comparing the fugacity of sulfur in smelters operating during a similar period, the range over which smelting was carried out

Table 6 Liquidus temperatures and oxygen and sulfur fugacities at which slag formation was possible at selected locations

Location	Time	Smelting/liquidus temperature [°C]	Temperature determination method	$\log P_{O_2}$ provided by the authors	Oxygen fugacity [$\log P_{O_2}$] Based on PADs*	Sulfur fugacity [$\log P_{S_2}$]
Polichno	Fifteenth to seventeenth century	1100–1200			−4.30 to −13.93	−2.50 to −6.59
Kondratów and Leszczyna, Poland [3]	Eighteenth to twentieth century	1210–1400	MELTS-Rhyolite software combined with geothermometers and petrological observations	QMF buffer no values given	−3.00 to −12.40	−3.87 to −5.77
Marsiliana, Italy [18]	Thirteenth to fourteenth century	1150–1300	Phase composition	no values given	−3.58 to −13.20	−1.87 to −7.68
Cabrières, France [2]	3rd millennium BC	1000–1200	Phase composition	at least -6	−4.30 to −15.57	−5.01 to −7.43
Crete [1]	Bronze Age	1150–1300	Phase diagrams	−7 to −9.5 (1300 °C)	−3.58 to −13.20	−4.81 to −6.21

*Fugacity has been calculated for the given liquidus temperatures

in Polichno is narrower than that in Marsiliana smelting and broader than the work carried out in Kondratów and Leszczyna (Table 6). The decreasing range of sulfur fugacity during the process may be due to the improvements in the production process between the thirteenth and twentieth centuries. The narrower range may result in better control of the ongoing process and, thus, better efficiency. The range of $\log P_{S_2}$ during smelting in Cabrières and Crete is narrower than in Polichno. At the same time, these locations are characterized by relatively low sulfur fugacity (Table 6). In the case of Crete, this is due to the use of mainly oxidized copper minerals during smelting [1]. In Cabrières, the smelting process was based on sulfide ore, and lower $\log P_{S_2}$ may suggest a less efficient ore enrichment process. The other explanation is the partial roasting of the ore, which may have been used at Cabrières before the actual smelting [2].

Importance of PADs in the O_2 and S_2 fugacity determinations

Based on the PAD, it is possible to determine several critical factors related to smelting. PADs directly give information on the fugacity of oxygen, sulfur, or other relevant components (e.g., arsenic) affecting the smelting process. With PADs, it is also possible to determine whether the smelting process was conducted under thermodynamic equilibrium conditions or measure how deeply non-equilibrium conditions existed. The occurrence of phases in the samples whose fields of occurrence in the diagram do not overlap indicates a thermodynamic non-equilibrium during smelting. The greater the distance between these fields, the more non-equilibrium conditions were. The best example is sample POL5, where PbO and FeS were found. Theoretically, these phases should not co-occur (Fig. 6). In such cases, the temperature and volatile composition most likely changed during crystallization.

Because oxygen fugacity is one of the most critical factors for metal production [3, 9, 17], it should be determined as accurately as possible. PADs make it possible to obtain more precise results compared to commonly used Fe buffers. This is because Fe buffers were designed for natural rocks and only consider the degree of Fe oxidation [21, 22]. Basing studies only on the degree of iron oxidation is understandable when analyzing crystallization processes in natural rocks but may be insufficient when for metallurgical slags. The feasibility of using Fe buffers requires information on the degree of iron oxidation in the samples. This information can be provided through analyses of the chemical composition of iron-containing phases or additional analyses using tools such as, e.g., Mössbauer spectroscopy [11, 14]. Historical metallurgical slags very often consist mainly of glassy phases, and crystalline phases occur only sporadically dispersed in the glass [1, 3, 25], which limits the possibility of determining the degree of Fe oxidation based on the phase composition of slags. Advanced petrological and chemical tools (like mentioned Mössbauer spectroscopy) are not commonly used for archaeological studies due to the limited availability of equipment. Due to the limitations in the use of Fe buffers, the use of PADs appears to be preferable because it is possible to consider all the phases that were observed in the samples (e.g., Cu, Pb, Zn, Fe) when creating the diagram, rather than being limited to Fe only.

Another advantage of PADs over Fe buffers is the ability to determine the fugacity of other furnace gases. Unlike Pb or Fe smelting, where the only relevant gaseous components are O_2, CO, and CO_2, the fugacity of sulfur (and/or arsenic) was equally important during copper production. Copper production in historical times was performed by producing a matte (sulfide melt), which was then processed to produce metallic copper. Matte production could only occur if the sulfur fugacity was sufficient to form sulfides. For this reason, when reconstructing historical processes, it is necessary to determine the P_{S2}, especially in copper smelting. It is impossible to determine it using Fe buffers. During copper production, it was crucial to maintain the right amount of sulfur in the system so that the matte contained as much Cu and as little Fe as possible. At the same time, care was taken to avoid oxidation of Cu, which would pass into the slag in the form of Cu_2O [12]. Former smelters were thus able to manipulate the efficiency of the process by the O_2 and S_2 fugacities during smelting. In addition to knowledge of conditions during smelting, analyzing the sulfur/oxygen fugacity allows us to answer the question of how much-developed technology was used by past metallurgists.

Ellingham diagrams can also determine the gas composition in historical processes [25]. Diagrams that consider the fugacity of oxygen during the oxidation of metallic phases are widely available in the literature [37]. We can also find diagrams from which we can read the fugacity of sulfur with the transition between metallic and sulfide phases [38]. The disadvantage of using Ellingham diagrams is that no single diagram simultaneously considers the fugacity of oxygen and sulfur. In addition, Ellingham diagrams most often consider too many phases in a single diagram, and their readability is limited. An additional advantage of PADs is that the thermodynamic equilibrium conditions directly between the sulfide and oxide phases can also be read from them (Fig. 6). Such transitions are not included in any of the available Ellingham diagrams.

Conclusions

Study proves that the PADs can be effectively applied during the reconstruction of the oxygen and sulfur fugacities during historical metallurgical processes. The diagrams made it possible to determine the oxygen and sulfur fugacities during copper smelting in Polichno. This was possible due to the determination of the slags' liquidus and solidus temperatures, which were then used for thermodynamic calculations. Combining the experimental smelting and high-temperature microscopic observations allowed for more precise solidus temperature determinations. Considering that sulfide ores were processed through the production of speiss/matte, both the oxygen and sulfur fugacity during smelting were determined. The oxygen fugacity during ores processing in Polichno ranges from $\log P_{O_2} = -4.30$ (POL1, POL4 at 1200 °C) to −14.08 atm. (POL3 at 1090 °C). The sulfur fugacity ($\log P_{S_2}$) ranged from −2.50 atm. (POL5 at 1200 °C) to −6.92 (POL4 at 1060 °C). The relatively high sulfur availability during smelting indicates using sulfide ores without roasting in Polichno. The wide range of sulfur and oxygen fugacity, in turn, indicates the heterogeneity of the process. Most often, oxidation–reduction conditions are determined by Fe buffers in reconstructions of historical metallurgical processes. Such treatment has restricted the possible calculation to Fe-containing phases only. It is better to consider the other elements occurring in the slags because determining the iron oxidation degree in slag samples can be problematic, especially for entirely glassy slags. PADs make it possible to consider those metals whose occurrence was confirmed during EPMA studies. An additional advantage of the presented method is the possibility of presenting the fugacity of sulfur and oxygen using a single diagram.

Supplementary Information

The online version contains supplementary material available at https://doi.org/10.1186/s40494-024-01171-y.

Additional file 1. Results of liquidus and solidus temperature determinations of slags from Polichno using high-temperature microscope observations

Additional file 2. Graphs showing the dependence of the equilibrium constant (logK) on temperature a) for oxides, b) for sulfides (made based on data from barin [31]).

Additional file 3. logK values used in thermodynamic calculations, and a summary of results on the equilibrium constant between the metallic and oxide-sulfide phases.

Acknowledgements
This study was supported by the National Science Center (NCN) Grant No. 2019/35/O/ST10/00313.

Author contributions
Conceptualization: KK, RW, and AG; Methodology: KK, RW, AG, PM, and MŚ; Writing—original draft preparation: KK; Writing—review and editing: KK, RW, and AG; Resources: KK and RW; Figures, tables, and Additional files: KK and RW. All authors read and approved the manuscript.

Funding
This research was funded by the National Science Center (NCN) Grant No. 2019/35/O/ST10/00313.

Data availability
The data that supports the finding of the study is given in the tables and figures within the main text and in Additional files. This study brought together existing data from several different sources, which are cited throughout. No dataset from external repositories was used in this study. All existing data used for this publication are cited in the reference section.

Code availability
Not applicable.

Declarations

Ethics approval and consent to participate
Not applicable.

Consent for publication
Not applicable.

Competing interests
The authors declare no competing interests.

Received: 15 December 2023 Accepted: 5 February 2024
Published online: 12 February 2024

References

1. Bassiakos Y, Catapotis M. Reconstruction of the copper smelting process based on the analysis of ore and slag samples. Hesperia Supplements. 2006;36:329–53.
2. Bourgarit D, Mille B, Prange M, Ambert P, Hauptmann A. Chalcolithic fahlore smelting at Cabrières: reconstruction of smelting processes by archaeometallurgical finds. Archaeometall Eur. 2003;1:431–40.
3. Derkowska K, Świerk M, Nowak K. Reconstruction of copper smelting technology based on 18–20th-century slag remains from the old copper basin, Poland. Minerals. 2021;11:926.
4. Ettler V, Červinka R, Johan Z. Mineralogy of medieval slags from lead and silver smelting (Bohutín, Příbram district, Czech Republic): towards estimation of historical smelting conditions. Archaeometry. 2009;51:987–1007.
5. Kądziołka K, Pietranik A, Kierczak J, Potysz A, Stolarczyk T. Towards better reconstruction of smelting temperatures: methodological review and the case of historical K-rich Cu-slags from the Old Copper Basin, Poland. J Archaeol Sci. 2020;118: 105142.
6. Kierczak J, Pietranik A. Mineralogy and composition of historical Cu slags from the Rudawy Janowickie Mountains, southwestern Poland. Can Mineral. 2011;49:1281–96.
7. Kupczak K, Warchulski R, Dulski M, Środek D. Chemical and phase reactions on the contact between refractory materials and slags, a case from the 19th Century Zn-Pb Smelter in Ruda Śląska, Poland. Minerals. 2020;10:1006.
8. Maldonado B, Rehren T. Early copper smelting at Itziparátzico, Mexico. J Archaeol Sci. 2009;36:1998–2006.
9. Warchulski R, Kupczak K, Gawęda A, Sitko R. Complete reconstruction of the process and conditions during gold smelting in the 15–17th century in Złoty Stok based on metallurgical slags. Archaeometry. 2022;64:916–34.

10. Warchulski R, Szczuka M, Kupczak K. Reconstruction of 16th–17th century lead smelting processes on the basis of slag properties: a case study from Sławków, Poland. Minerals. 2020;10:1039.
11. Warchulski R. Zn-Pb slag crystallization: evaluating temperature conditions on the basis of geothermometry. Eur J Mineral. 2016;28:375–84.
12. Davenport WG, King M, Schlesinger M, Biswas AK. Extractive Metallurgy of Copper. 2002:1–460.
13. Hauptmann A, Rehren T, Schmitt-Strecker S. Early Bronze Age copper metallurgy at Shahr-i Sokhta (Iran) reconsidered. Bochum: Deutsches Bergbau-Museum; 2003. p. 197–213.
14. Nakanishi A. Mössbauer study of ancient iron smelting slag in Japan. Hyperfine Interact. 2008;186:135–9.
15. Cabała J. (in Polish) Heavy metals in the soil environment of the Olkusz Zn-Pb ore mining district. Katowice: Wydawnictwo Uniwersytetu Śląskiego; 2009. p. 1–132.
16 Agricola G. (in Polish) On the nature of metals (De Re Metallica. Jelenia Góra: Muzeum Karkonoskie w Jeleniej Górze; 2000. p. 1–531.
17. Giacometti F, Rebay G, Riccardi MP, Tarantino SC, Cucini TC, Tizzoni M. Iron Age silicate slags from Val Malenco (Italy): the role of textural and compositional studies in the reconstruction of smelting conditions. Periodico di Mineralogia. 2014;83:329–44.
18. Manasse A, Mellini M. Chemical and textural characterisation of medieval slags from the Massa Marittima smelting sites (Tuscany, Italy). J Cult Herit. 2002;3:187–98.
19. Nezafati N, Pernicka E. Early silver Production in Iran. Iranian Archaeology. 2012:10.
20. Ströbele F, Wenzel T, Kronz A, Hildebrandt LH, Markl G. Mineralogical and geochemical characterization of high-medieval lead–silver smelting slags from Wiesloch near Heidelberg (Germany)—an approach to process reconstruction. Archaeol Anthropol Sci. 2010;2:191–215.
21. Lindsley DH. Oxide minerals: petrologic and magnetic significance. Berlin: Walter de Gruyter GmbH & Co KG; 2018. p. 1–10.
22. Zhao D, Essene EJ, Zhang Y. An oxygen barometer for rutile–ilmenite assemblages: oxidation state of metasomatic agents in the mantle. Earth Planet Sci Lett. 1999;166:127–37.
23. Report on the state of the Chęciny commune for 2021. 2022:1–90
24 Paulewicz M. (in Polish) Chęciny ore mining (14th to mid–17th century. Kielce: Kieleckie towarzystwo naukowe; 1992. p. 1–155.
25. Kupczak K, Warchulski R, Gawęda A. Reconstruction of smelting conditions during 16th-to 18th-century copper ore processing in the Kielce region (Old Polish Industrial District) based on slags from Miedziana Góra, Poland. Archaeometry. 2023;65:547–69.
26. Geoportal. n.d. https://www.geoportal.gov.pl. Accessed 3 Jan 2023.
27. Długosz J, (in Polish) Annals or chronicles of the famous Kingdom of Poland. Book 1. 1455–1480:169
28. Gałuszka A, Migaszewski ZM, Dołęgowska S, Michalik A, Duczmal-Czernikiewicz A. Geochemical background of potentially toxic trace elements in soils of the historic copper mining area: a case study from Miedzianka Mt., Holy Cross Mountains, south-central Poland. Environ Earth Sci. 2015;74:4589–605.
29. Siuda R, Domańska-Siuda J. STOP 1: Miedzianka deposit—one of the oldest mining centres in Poland. Proceedings of the XXVIth Meeting of the Petrology Group of the Mineralogical Society of Poland. 2019;99–103.
30. Ciurej A, Struska M, Wolska A, Chudzik W. The Miedzianka Mountain Ore Deposit (Świętokrzyskie Mountains, Poland) as a site of historical mining and geological heritage: a case study of the Teresa Adit. Minerals. 2021;11:1177.
31. Kowalczewski Z, Szczecińska A. (in Polish) Results of research on slags from several sites of former non-ferrous metallurgy in the Holy Cross Mountains. Rocznik Świętokrzyski. 1977;5:151–68.
32. Pang CH, Hewakandamby B, Wu T, Lester E. An automated ash fusion test for characterisation of the behaviour of ashes from biomass and coal at elevated temperatures. Fuel. 2013;103:454–66.
33. Barin I. Thermochemical data of pure substances. VCH. 1993;2:1523
34. Muan A, Osborn EF. Phase equilibria among oxides in steelmaking. Massachusetts: Addison-Wesley publishing company, INC; 1965. p. 113.
35. Jak E, Hayes P, Pelton A, Decterov S. Thermodynamic modelling of the A12O3-CaO-FeO-Fe2O3-PbO-SiO2-ZnO system with addition of K and Na with metallurgical applications. In Proc VIII Int'l Conf on Molten Slags, Fluxes and Salts; Santiago, Chile. 2009:473–90
36. Westner KJ, Klein S, Sergeev D, Müller M. Temperature estimates of historical Pb-Ag smelting slags: a multi-methodological approach. J Archaeol Sci Rep. 2022;46: 103654.
37 Hasegawa M. Ellingham diagram. Treatise on process metallurgy. Amsterdam: Elsevier; 2014. p. 507–16.
38. Shatynski SR. The thermochemistry of transition metal sulfides. Oxid Met. 1977;11:307–20.

Publisher's Note